DOR: 20.1001.1.27170314.2023.12.1.1.4

Research Paper

Investigating the Effect of Residual Stress on Fatigue Crack Propagation by Modified J-integral and Experimental Method

Ali Moarrefzadeh[1*], Shahram Shahrooi[2]

[1]Department of Mechanical Engineering, Mahshahr Branch, Islamic Azad University, Mahshahr, Iran

[2]Department of Mechanical Engineering, Ahvaz Branch, Islamic Azad University, Ahvaz, Iran

*Email of Corresponding Author: a_moarrefzadeh@yahoo.com

Received: December 20, 2022; Accepted: February 25, 2023

Abstract

This paper is introduced new method for predicting of fatigue crack propagation (FCP) in residual stress (RS) field due to welding. If there is stress in the material and is subjected to loading, the effects of loading and RS must be considered simultaneously. For this purpose, stress intensity factor (SIF) in liner elastic fracture mechanics (LEFM) approach and J-integral in elastic-plastic fracture mechanics (EPFM) approach are used. The superposition principle based on LEFM is used to consider the RS effects on the cycle ratio and SIF. To achieve more appropriate results based on EPFM, the J-integral is modified to consider the simultaneous effects of RS and external loading. Finally, the FCP equations are modified to consider into calculation the simultaneous influences of RS and cyclic loading. Results from FCP equation based on J-integral are in good agreement with experimental results. The obtained results show that the MLPG method is suitable for calculating the residual stress and the modified J-integral method is the best method for predicting FCP in the RS field caused by welding.

Keywords

Residual Stress, Welding, Stress Intensity Factor, J-integral, Fatigue Crack Propagation

Abbreviation

a	Crack length
E	Elasticity module
G	Shear module
K	Stress intensity factor
R	Cycle ratio
σ_{res}	Residual stress
$\sigma_{\max}, \sigma_{\min}$	Minimum and maximum stresses
Ω	Problem domain
ϕ_i	Shape function

1. Introduction

Numerical methods have a great ability to solve engineering problems. The finite element method (FEM) is a very strong method to solve problems numerically. In FEM, the problem model is divided into smaller parts. In this numerical method, for each of these small parts, the differential equation, becomes a linear algebraic equation. FEM has been employed to calculate the RS and thermal stress due to the welding processes [1-4]. Wu et al. [5] calculated the influences of welding RS on crack growth. They used the FEM for calculation of the cycle ratio and FCP rate. Itoh et al.[6], investigated the temperature field created by welding and then obtained the sum of the displacements due to the thermal loading to calculate the RS. Teng et al. [7] used FEM for two-dimensional modeling to calculate RS due to multi-pass butt-welds. Bao et al. [8] investigates the temperature field and RS due to welding by FEM. Also, they calculated SIF in the RS field. Seifi [9] investigated the effects of RS on fracture parameters for welded cracked samples. For this purpose, the FEM and J-integral method was used.

In recent years, a new numerical method has been introduced to solve problems, which, unlike the FEM, does not require problem domain meshing to solve the problem. This method is called Meshless Local Petrov-Galerkin (MLPG) method. In this numerical method, the whole model of the problem, including the inside and its boundaries, is defined using the distribution of nodes with arbitrary scatter. Moarrefzadeh et al[10,11] used the MLPG method based on LEFM for the prediction of the FCP in the welding RS field. They used the MLPG formulation based on the Moving Least Square (MLS) method to interpolate the displacement field due to RS and external loading. Also, they calculated SIF for the RS and cyclic loading. The results of the prediction based on their research were very close to the laboratory results for small crack length.

In the elastic case, to study the displacement and stress field, the LEFM approach provides acceptable results. This approach can be used for the calculation of the SIFs due to the RS and external stress[12-14]. In the elastic-plastic case, this method does not give good results. EPFM must be used if there is significant plastic deformation and RS at the crack tip. Under these conditions, the behavior of the crack can be predicted by the J-integral method [15-18].

In this paper, the SIF based on the LEFM approach has been calculated to predict crack behavior in the RS field. Then, to get a more accurate prediction of the FCP rate in the RS field, the J-integral method has been used. In this regard, J-integral has been modified to estimate the crack behavior in the case of significant plastic deformation due to external loading and RS. The results obtained with this method-based EPFM are more accurate than the LEFM approach and are closer to the experimental results. The results show that the modified walker equation is satisfactory for the prediction of FCP. Also, the results show that the modified J-integral can be used to predict the FCP in the RS field caused by welding.

2. Materials and sample

In this study according to ASTM standards, the two stainless steel 304 plates with a thickness of 2mm, length of 300mm, and width of 150mm according to Figure 1(a) are welded together butt joint. For this purpose, the TIG welding process according to Figure 1(b) is employed. For the calculation of the temperature field, transferred heat of Q=110J/mm and welding time of t=90s are considered for welding conditions.

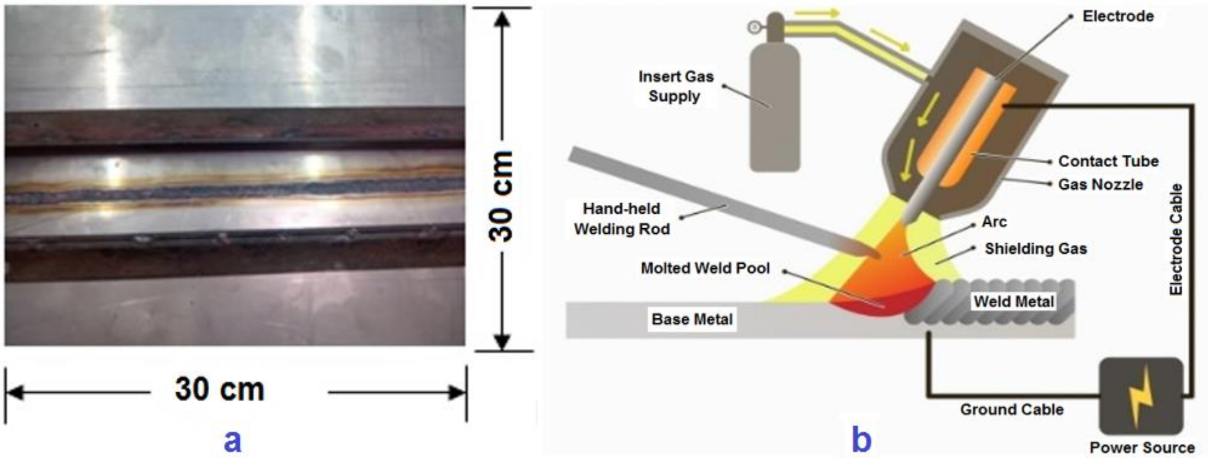

Figure 1. a) Dimensions of the welded specimen b) b TIG welding process

According to Figure 2. the Hole-Drilling Strain-Gage method based on the ASTM E837 standard[19], is also used to measure the residual stress.

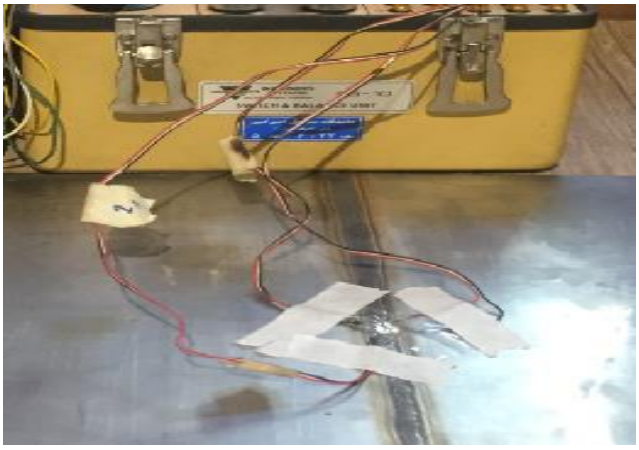
Figure 2. The Hole-Drilling Strain-Gage method

To study the crack behavior in the presence of residual stresses, a crack of length 2a is considered perpendicular to the welding direction. The required mechanical properties of stainless steel 304 are shown in Table 1.

Table1. Mechanical properties

σ_y (MPa)	K_{IC} $(MPa\sqrt{m})$	E (GPa)	υ
265	219	206	0.29

Where σ_y, K_{IC}, E and υ are yield stress, elastic modulus, fracture toughness, and Poisson ratio, respectively.

3. Calculation of SIF

3.1. Calculation of the SIF without RS

The first mode of displacement and stress distribution based on LEFM is calculated by[4]:

$$\sigma_{ij} = \frac{K_I}{\sqrt{2\pi r}} f_{ij}(\theta) \qquad (1)$$

$$u_i = 2(1+\upsilon)\frac{K_I}{E}\sqrt{\frac{r}{2\pi}}\, g_i(\theta) \qquad (2)$$

Where r and θ are the radial distances from the crack tip and the angle of the crack direction are counter-clockwise, respectively. K_I is SIF of mode I and $f_{ij}(\theta)$, $g_i(\theta)$ are the trigonometric functions for this fracture mode. The stress distribution is obtained by the MLPG method [11] according to Figure 3. These results indicate a redistribution of stress due to crack growth.

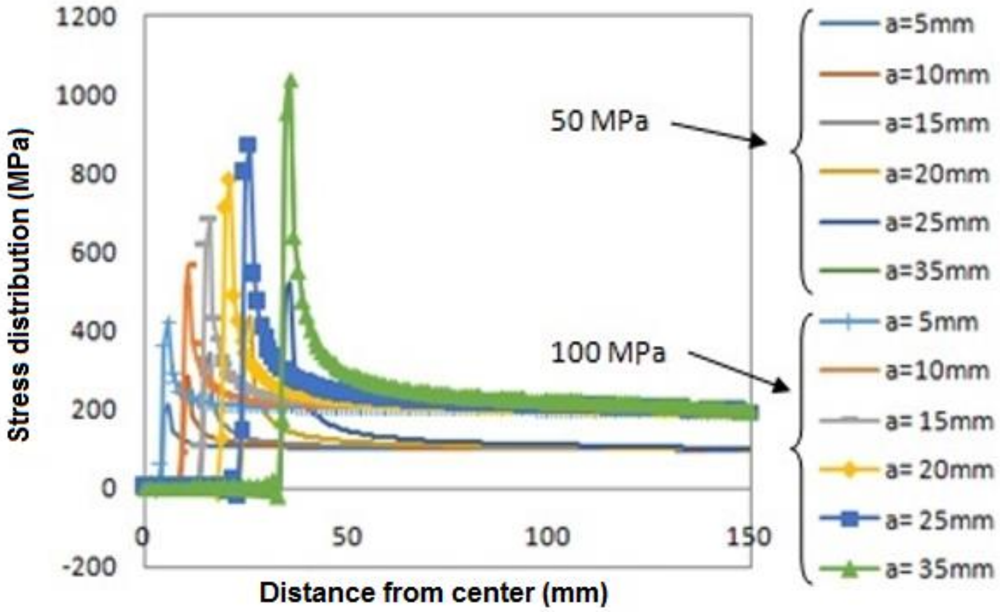

Figure 3. Stress variations with crack growth

3.2. The SIF in the RS field

The SIF due to the RS field (K_{res}) based on the weight function method is obtained by[4]:

$$K_{res} = \int m(x,a)\sigma_{res}(x)dx \qquad (3)$$

where $m(x,a)$ is weight function that defined as follows[4]:

$$m(a,x) = \sqrt{\left(\frac{a}{\pi(a^2 - x^2)}\right)} \qquad (4)$$

Also, $\sigma_{res}(x)$ is longitudinal RS distribution for the model without crack[12]:

$$\sigma_{res}(x) = \sigma_{\max} \exp\left(\frac{-x^2}{2\hbar^2}\right)\left[1 - \left(\frac{x}{\hbar}\right)^2\right] \qquad (5)$$

where $\sigma_{\max}$ is the maximum RS in the line of weld and according to Figure 4, $2\hbar$ and x, are the size of the tension zone and the vertical distance from the weld line, respectively. By imposing Eq.(4) and Eq.(5), into Eq.(3), K_{res} is determined:

$$K_{res} = \sigma_{\max} \exp(-0.42(\frac{a}{\hbar})^2)\left[1-\frac{1}{\pi}(\frac{a}{\hbar})^2\right]\sqrt{\pi a} \qquad (6)$$

The MLPG method[10] based on thermo-elastoplastic equations according to Figure 4 has been used for the numerical calculation of RS. For validation of numerical results, the Hole-Drilling Strain-Gage method was used. As shown in Figure 4, the results of the MLPG method and the results of the hole-drilling method are very close to each other.

Figure 5 compares the stress distribution in different cases. First, the distribution of longitudinal RS in the direction perpendicular to the weld line is shown. Then its redistribution is shown by crack length a=5mm, which shows that crack growth leads to a change in the RS distribution. Also, the distribution of longitudinal stress is plotted around the crack without residual stress.

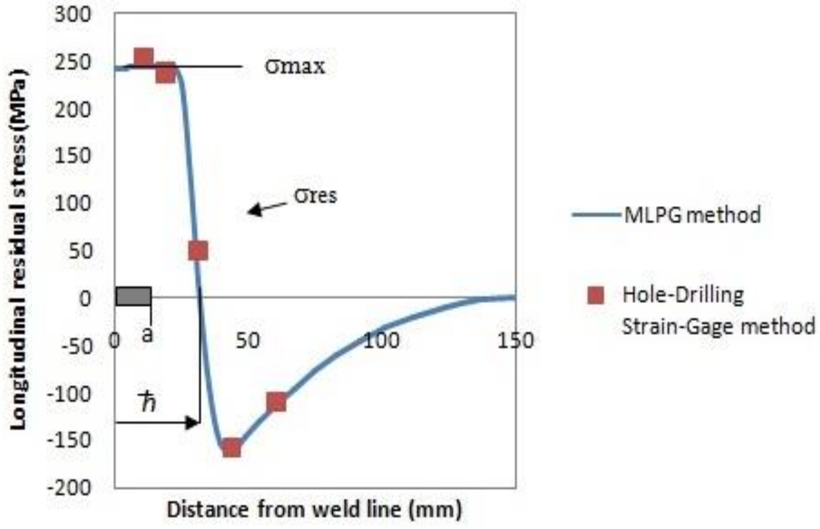

Figure 4. Longitudinal RS distribution

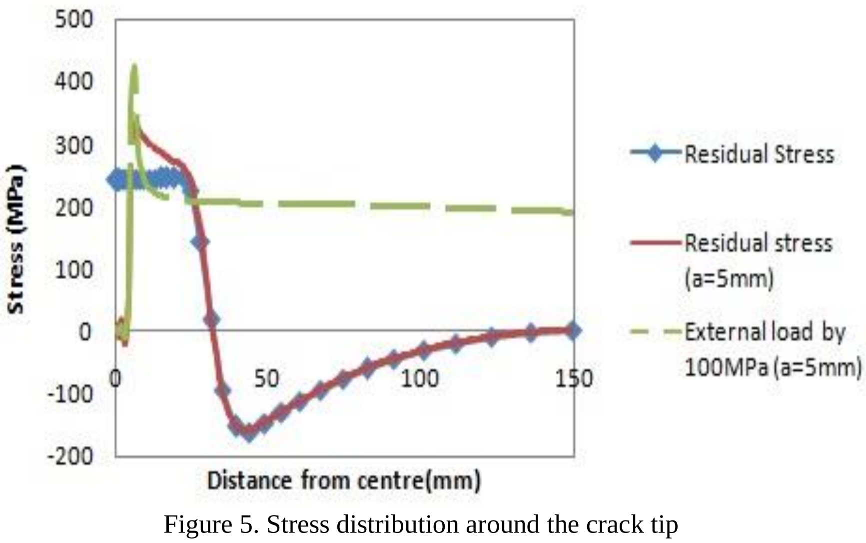

Figure 5. Stress distribution around the crack tip

4. The J-integral method

4.1. Methodology

The J-integral presents a way to calculate the rate of strain energy release, or energy per unit fracture surface area, in a material. If the size of the plastic area created at the crack tip is large enough that it is not small compared to the crack length, G, can not be obtained based on the field of elastic stress. In this case, the determination of G is based on the specifications of the plastic area of the crack tip. Therefore, Elastic-plastic behavior is not available. Since the effects of the plastic size of the crack tip can not be ignored, the J-integral method can be used to determine the amount of G. In this regard, the LEFM approach can not be valid for plastic deformation. Therefore, the EPFM approach must be used. For elastic-plastic deformation J-Integral based on this approach can be used. The local value of the G rate in a sample point can be written as[9]:

$$J = \lim_{\Gamma \to 0} \int_{\Gamma} (W n_1 - \sigma_{ij} \frac{\partial u_j}{\partial X_j} n_i) d\Gamma = \int_{\Gamma} (W \delta_{1i} - \sigma_{ij} \frac{\partial u_j}{\partial X_j}) n_i q d\Gamma \qquad (7)$$

Where, Γ is a surrounding of the curve the point in a plane vertical to crack front according to Figure 6. $\vec{n}$ is a unit normal vector on Γ. U is the displacement component, σ is the tensor of stress, W is the strain energy density and q is the weight function that is used to eliminate the limitation. when there are no RS and body force in materials, Eq.(7) can be used for the 2D problem as[9]:

$$J = \int_{\Gamma} (\sigma_{ij} \frac{\partial u_j}{\partial X_j} - W \delta_{1i}) \frac{\partial q}{\partial X_j} d\Gamma \qquad (8)$$

Based on Figure 6, this integral is defined as changes in potential energy, V, by crack growth da[9]:

$$J = -\frac{\partial V}{\partial a} \qquad (9)$$

4.2. J-integral calculation in the residual stress field

If residual stresses are considered around the crack front, this equation is path dependent.

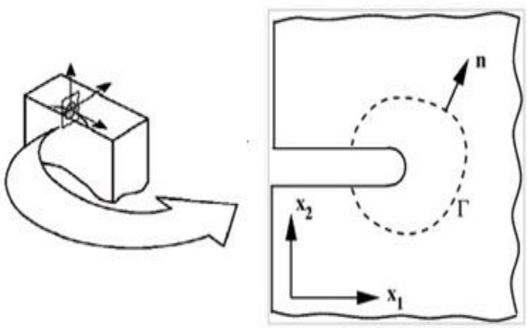

Figure 6. J-integral parameters

Therefore, it can not be used as a fracture parameter. When there is residual stress in materials, displacement gradients are depending on external loading and residual stress. Also, initial strain due to residual stresses changes the strain energy density. The mechanical strain, ε_{ij}^{m}, and density of strain energy, W, can be presented by Eqs(10) and (11).

$$\varepsilon_{ij}^{m} = \varepsilon_{ij}^{e} + \varepsilon_{ij}^{p} - \varepsilon_{ij}^{in} \qquad (10)$$

$$W = \int_0^{\varepsilon} \sigma_{ij} d\varepsilon_{ij}^{m} = W^t - W^{in} \qquad (11)$$

Where, $\varepsilon_{ij}^{e}, \varepsilon_{ij}^{p}, W^{t}$ and W^{in} are elastic strain, plastic strain, total strain energy density, and initial strain energy density respectively. According to this definition, Eq.(8) for calculation of J-Integral due to RS and external stress can be written as[9]:

$$J = \int_A \sigma_{ij} \left(\frac{\partial u_j}{\partial X_1} \frac{\partial q}{\partial X_i} + \frac{\partial \varepsilon_{ij}^{in}}{\partial X_1} q \right) - (W^t - W^{in}) \frac{\partial q}{\partial X_1}) dA \qquad (12)$$

Including this equation is to calculate the J-integral by considering the simultaneous effects of initial strain, thermal strain, and RS in the problem. To investigate the RS effects on crack growth in the elastic-plastic case, the EPFM approach was applied for modified J-integral calculation due to the external stress and RS. Figure 7 shows how the J-integral changes with different external loads. Results of modified J-integral according to Eq.(12) for residual and external stress were plotted in Figure 8. When martial has residual stresses, the J-integral values change by these stresses. Tensile RS leads to an increase and compressive leads to a decrease of J-integral values. Variations of J-integral were changed when the external load was subjected to the workpiece. In this figure, the J-integral in the sample without RS as well as the integral due to RS are shown separately. Therefore, the difference in these curves is due to the presence of residual stress. As it is known, the J-integral in the sample with tensile residual stress has larger values than the sample without residual stress. Therefore, the growth rate of fatigue crack changes.

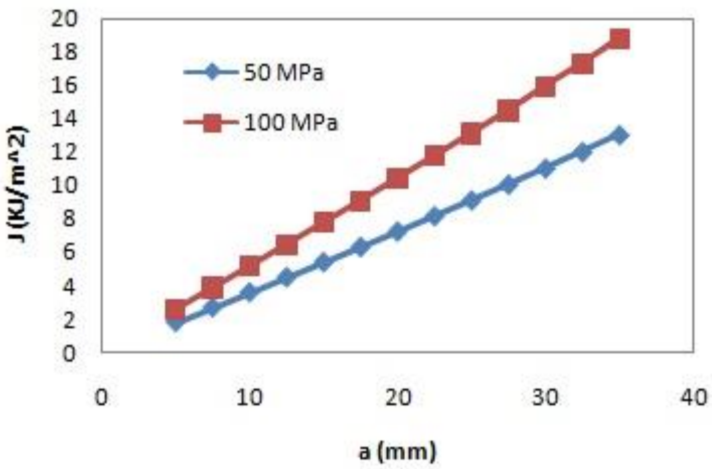

Figure 7. External load variations by J-integral

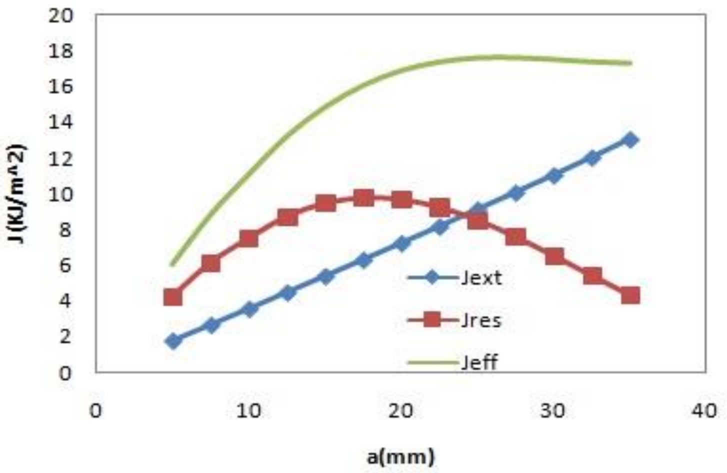

Figure 8. J-integral results for external load and residual stress

5. The Fatigue crack propagation

5.1. FCP in the residual stress field

The SIF based on the LEFM approach is enough factor to explain the stress distribution at the crack tip. If the size of the plastic area is small relative to the length of the crack, the SIF can be used for the calculation of the stress around the crack tip.

The Walker equation for this purpose is as[20]:

$$\frac{da}{dN} = c\{(K_{\max} - K_{\min})[1 - R_{eff}]^{\mu-1}\}^{n} \qquad (13)$$

where c, n and μ are material constants. $K_{\max}$ *and* $K_{\min}$ are minimum and maximum SIF. Also, the effective cycle ratio (R_{eff}) is defined by:

$$R_{eff} = \frac{K_{\min} + K_{res}}{K_{\max} + K_{res}} \qquad (14)$$

The SIF based on the elastic-plastic case is not enough to factor to explain the stress distribution at the crack tip. Therefore, the J-integral based on EPFM must be used instead of SIF in the equation of the FCP rate. To evaluating of FCP in these cases EPFM approach must be used. For this purpose, the cyclic of J-Integral can be employed for considering the elastic-plastic deformation around the crack:

$$\frac{da}{dN} = f(\Delta J) \qquad (15)$$

Where ΔJ are variations of the J-integral cyclic. Fatigue crack propagation equation based on cyclic J-integral can be written for elastic-plastic deformation around crack as follows:

$$\frac{da}{dN} = c(\Delta J_{eff})^{n} \qquad (16)$$

Where, ΔJ_{eff}, according to Eq.(12) includes initial strain, thermal strain, and RS.

5.2. Experimental results and validation of predicting FCP rate

The FCP equation according to Eq.(13) based on LEFM and FCP equation according to Eq.(16) based on J-integral were employed to predict the FCP rates. For this purpose, $C = 6\times10^{-12}$, $n = 3.067$ and $\mu = 0.5$ are considered[21].

Residual stresses affect the FCP rate. This effect is applied to the cyclic stresses and the results of the minimum and maximum SIF are very significant for the laboratory sample that is removed from the residual stress material to test fatigue. To study the fatigue test based on the ASTM E647 standard [22], an initial crack must be created. Electric discharge machining was used to create the initial notch. To create the initial crack from the notch, the sample is subjected to cyclic loading. Cyclic loading is applied symmetrically on the machined notch with the maximum SIF with tolerance $\pm 5\%$. The maximum SIF should not exceed the maximum stress intensity factor to test the FCP rate. For this purpose, the rate of FCP has been less than $10^{-8}\, m/cycle$ used. FCP test was performed with a Dartec fatigue test machine with a capacity of 50KN and 100Hz according to Figure 9 with a constant amplitude to check the fatigue crack growth. Cyclic loading according to Figure 9 with constant amplitude is applied symmetrically on the crack in the environment with maximum temperature of 25 ° C and humidity of 25%, cycle ratio R = 0.5 and frequency of 15 Hz. Monitoring and measuring crack growth in the FCP test, it has been done visually by accurately increasing the crack length $\Delta a = 0.25mm$ by sensitive and accurate cameras.

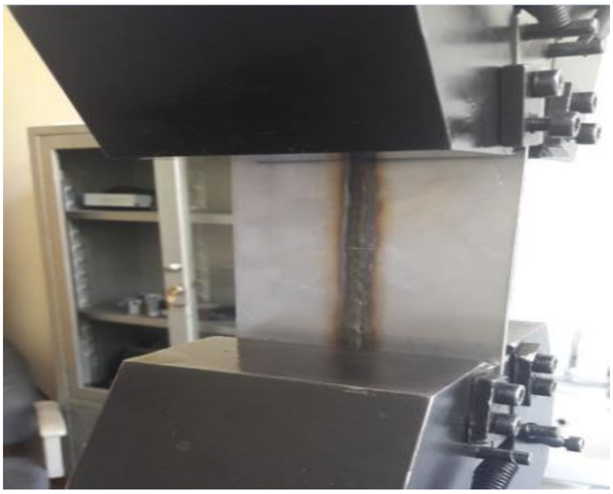

Figure 9. Expermental model for fatigue crack propagation test

Figure 10 shows the calculated FCP rates by modified equations for R=0.5 and experimental test. The modified Walker equation shows close results with experimental results for $a \le 20mm$. When a >20mm this equation has not accurate enough. The main reason for the error of the results is that the size of the plastic zone of the crack tip is larger than the length of the crack. Therefore, the LEFM approach is not suitable when $a > 20mm$. FCP equation that modified by J-integral based on EPFM give good prediction for all crack sizes.

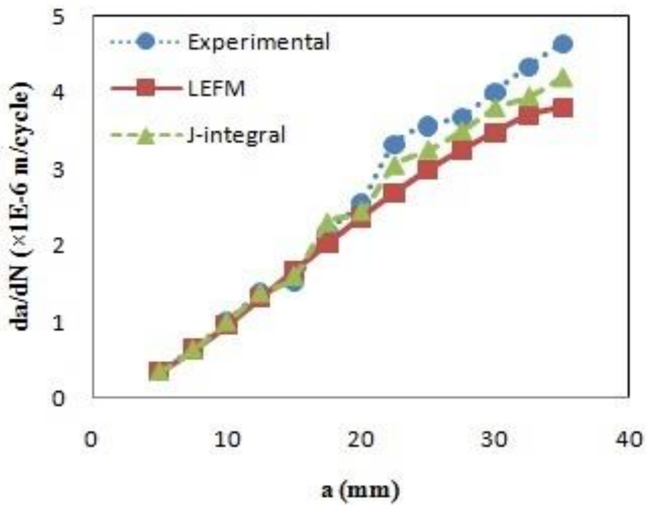

Figure 10. Results of numerical and experimental FCP

Figure 11. investigates the influences of RS on the FCP rate. The changes of FCP rate are shown for crack lengths from 5 mm to 35 mm. Also, the FCP rate is predicted for different cases. How FCP rates change due to residual stress is well illustrated.

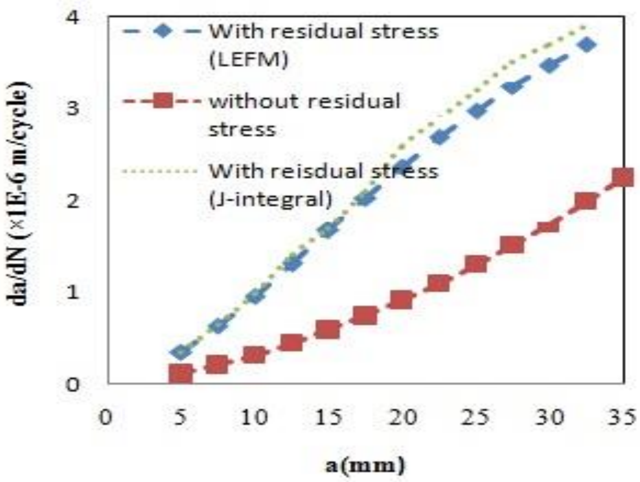

Figure 11. Influences of residual stress on FCP

6. Conclusion

To achieve a new method in fracture mechanics, a new method based on J- integral was presented that investigated the RS influences on the FCP rate. The J-integral equation in the RS field to consider the influences of this stress on crack behavior has been modified in order to get more correct results. The results are as follows:

1. The comparison of the results shows that the numerical simulation results are in good agreement with the experimental results (about 10%) in calculating the residual stress.
2. A new formulations based on J-integral to consider RS has been proposed.
3. When material has RS, the SIFs based on LEFM approach for small crack length and J-integral based on EPFM for all crack sizes are suitable to use. Modified J-integral evaluates the RS effects on FCP rate correctly. This formulation can be employed for investigation of the crack behavior in elastic and elastic-plastic cases.

4. The accuracy of the modified FCP equation based on J-integral to predict the amount of FCP in the presence of RS is well illustrated compared to the FCP equation based on SIF.

7. References

[1] Zubairuddin M., Albert S.K., Vasudevan M., Mahadevan S., Chaudhari V. and Suri V.K. 2017. Numerical simulation of multi-pass GTA welding of grade 91 steel. Journal of manufacturing process. 27:87–97.

[2] Muzamil M., Akhtar M., Samiuddin M., Mehdi M. 2016. Effect of heat treatment on impact resistance of AU5GT and AS7G06 aluminum alloys. Journal of Mechanical Science and Technology. 30: 4543–4548.

[3] Spaniel M., Jurenka H., Kuzelka J. 2009. Verification of FE model of fatigue crack propagation under mixed mode conditions. Meccanica. 44:189-195

[4] Ismail, A.E., Ariffin A.K., Abdullah S.A. and Ghazali, M.J. 2012. Stress intensity factors foe surface cracks in round bar under single and combined loadings. Meccanica. 47:1141-1156

[5] Wu, X. and Carlsson, J. 1984. Welding Residual Stress Intensity Factors for Half- Elliptical Surface Cracks in thin and thick Plates, Engineering Fracture Mechanics. 19(3):407-426.

[6] Itoh Y. and Suruga C. 1989. Prediction of Fatigue Crack Growth Rate in Welding Residual Stress Fields, Engineering Fracture Mechanics. 33:397-407.

[7] Teng L. and Lin C.H. 1998. Effect of welding conditions on residual stresses due to butt welds, International Journal of Pressure Vessels and Piping. 75:857-864.

[8] Bao R., Xiang Z. and Norvahida, A. 2010. Evaluating stress intensity factors due to weld residual stresses by the weight function and finite element methods. Engineering Fracture Mechanics. 7:2550–2566.

[9] Seifi, R. 2011. Effect of residual stress on fracture parameters of through cracks in welded plates. Procedia Engineering. 10:1895-1900.

[10] Moarrefzadeh A., Shahrooi S. and Jalali Azizpour M. 2019. The application of the meshless local Petrov-Galerkin method for the analysis of heat conduction and residual stress due to welding. The International Journal of Advanced Manufacturing Technology. 104: 723-742.

[11] Moarrefzadeh, A., Shahrooi S. and Jalali Azizpour M. 2019. Predicting fatigue crack propagation in residual stress field due to welding by meshless local Petrov-Galerkin method. Journal of Manufacturing Processes. 45: 379-391.

[12] Wu, X.R. and Carlsson J. 1984. Welding Residual Stress Intensity Factors for Half- Elliptical Surface Cracks in thin and thick Plates. Engineering Fracture Mechanics. 19(3): 407-426.

[13] Wu, X.R. 1984. The Effect of Welding Residual Stress on Brittle Fracture of Plates with Surface Cracks, Engineering Fracture Mechanics. 19(3): 427-439.

[14] Beghini, M. and Bertini L. 1990. Fatigue Crack Propagation through Residual Stress Field with Closure Phenomena, Engineering Fracture Mechanics. 36(3): 379-387.

[15] Qi, D.M. 1992. Recommendations on the Treatment of Residual Stresses in PD6493 for the Assessment of the Significance of Weld Defects. Engineering Fracture Mechanics. 41(2): 257-270.

[16] Finch, D.M. and Burdekin F.M. 1992. Effect of welding residual stress on significance of detects in various type if welded joints, Engineering Fracture Mechanics. 41(5): 721-735.

[17] Finch D.M. 1992. Effect of Welding Residual Stress on Significance of Defects in Various Types of Weld Joints, Engineering Fracture Mechanics. 42(3): 479-500.

[18] Meith, W.A. and Hill M.R. 2002. Domain-independent values of the J-integral for cracks in three-dimensional residual stress bearing bodies. Engineering Fracture Mechanics. 69: 1301-1314.

[19] ASTM Standard E837-01. 2013. Standard Test Method for Determining Residual Stress by the Hole-Drilling Srain-Gauge Method. Annual Book of ASTM Standards. ASTM International, West Conshohoken, PA.

[20] Glinka G. 1979. Effect of residual stress on fatigue crack propagation in steel weldments under constant and variable amplitude load in Fracture mechanics, ASTM STP 677, American society of testing and materials, 198-214

[21] Yahiaoui B., Petrequim P. 1974. Teude de la propagation de fissures par fatigue dans de aciers anoxyydabels austenitiques a bas carbon due type 304L and 316L. Review Physics Application (France). 9(4): 683-690.

[22] ASTM Standard E647-05. 1998. Standard Test Method for Measurement of Fatigue Crack Growth Rates, Annual Book of ASTM Standards, ASTM International, West Conshohoken, PA.